Original Article

Finite Element Analysis of Optimal Design of Distal Geometry of Cementless Femoral Prosthesis

Y Zhao, L Wang, Y Bao[1], R Xu[1], S He

Department of Orthopaedics, The Affiliated Suzhou Science and Technology Town Hospital, Nanjing Medical University Suzhou, Jiangsu, [1]Department of Aerospace Manufacturing Engineering, College of Mechanical and Electrical Engineering, Nanjing University of Aeronautics and Astronautics, PR China

Dr. Zhao and Dr. He contributed equally to this work and should be considered as equal first authors.

Received: 15-Oct-2021;
Revision: 21-Jan-2022;
Accepted: 31-Jan-2022;
Published: 22-Sep-2022

ABSTRACT

Aim and Background: This study aims to improve the geometric design of the distal cementless femoral prosthesis stem, thereby changing the stress distribution of the femoral prosthesis and reducing the proximal stress shielding and distal stress concentration of the femur, so as to obtain better bone growth and long-term stability. **Materials and Methods:** Two geometric shapes of the femoral stems, namely, inverted hollow cone and cross-shaped bottom groove, are designed for the distal femoral prosthesis. The model is built based on the femoral computed tomography (CT) data of healthy volunteers, and the finite element method is used to analyze and calculate the stress distribution of the two femoral prosthesis stems. **Results:** According to the length and width of bottom "cross" groove, the stress values of the femoral region of the cross-grooved distal femur are divided into five groups, namely, group 1 (length 1:1, groove width 1.0 mm); group 2 (length 1:1, groove width 1.5 mm); group 3 (length 1:1, groove width 2.0 mm); group 4 (length 1:2, groove width 1.0 mm); group 5 (length 1:2, groove 1.5 mm wide). And the non-grooved group of the distal femur is designated as group 0. In the segment A, B, and C of the femoral region, the difference in the mean stress between group 0 and groups 1, 2, and 3 have statistical significance. **Conclusion:** The bottom "cross" groove of the distal femoral prosthesis can change the stress distribution in the prosthesis-distal femoral region and reduce the stress concentration at the distal prosthesis. Wherein, the grooved design of length ratio 1:1 is more advantageous.

KEYWORDS: *Cross groove, distal femoral prosthesis, finite element analysis, taper hole, total hip replacement*

INTRODUCTION

The aging population is becoming more and more severe, and the number of patients with hip joint retrogression, inflammatory arthritis, and femoral neck fractures is gradually increasing. Total hip arthroplasty has become an effective treatment method and means for hip joint diseases.[1] The service life of a hip prosthesis is generally 15–20 years.

There are many factors that affect the life of hip prostheses, such as prosthetic materials, mechanical design, and prosthetic surface treatment. In addition, postoperative infection of hip surgery, prosthesis fracture, wear debris, and stress shielding can cause bone loss around the prosthesis, which will loosen the prosthesis and affect its service life.[2] Many scholars believe that the stress shielding of the hip joint prosthesis to the femur is the main cause of the aseptic loosening of the prosthesis.[3] Aseptic loosening is also the main reason for the revision of joint prostheses.[4-6] Some scholars believe that the stress shielding of the prosthesis to the femur is mainly due to the inconsistent elastic modulus of the metal prosthesis and the femur.[7] At present, the main materials used in the femoral stems of artificial

Access this article online

Quick Response Code:

Website: www.njcponline.com

DOI: 10.4103/njcp.njcp_1888_21

Address for correspondence: Dr. S He, Department of Orthopaedics, The Affiliated Suzhou Science and Technology Town Hospital, Nanjing Medical University Suzhou, Jiangsu PR China.
E-mail: hsjian.ok@163.com

How to cite this article: Zhao Y, Wang L, Bao Y, Xu R, He S. Finite element analysis of optimal design of distal geometry of cementless femoral prosthesis. Niger J Clin Pract 2022;25:1476-83.

hip joint prosthesis are titanium alloys, cobalt alloys, and medical stainless steels, and the femoral stems all use solid materials. Compared with human bones, these materials have great rigidity and low elastic modulus.[8] After the artificial joint is implanted in the human body, the huge difference in stiffness between itself and the human bone will cause stress shielding, resulting in bone loss, and eventually may cause serious complications such as artificial joint loosening or bone fracture.[9,10] In addition, the geometric design of the femoral prosthesis is also one of the factors that affect the stress shielding of the femoral prosthesis.[11,12] Therefore, optimizing the contact stress distribution between the femur and the hip joint prosthesis is one of the main directions of hip joint design.[13-15]

The purpose of this study is to optimize the design of the distal femoral prosthesis, hoping to reduce the stress concentration on the femoral inner wall of the distal femoral prosthesis and increase the stress of the proximal femur by changing the geometry of the distal femoral prosthesis. The optimal design schemes for the geometric shape of the distal femoral prosthesis stem in this study are as follows: 1. hollow cone design of the distal femoral prosthesis stem; 2. cross groove design of the distal femoral prosthesis stem (different groove width and length ratios are analyzed separately), and this paper combines the computed tomography (CT) technology, computer-aided design, and three-dimensional finite element analysis methods to explore the influence of these design schemes on the stress of femoral prosthesis and its distribution, thus providing the theoretical basis and reference for the optimal design of the femoral prosthesis.

Materials and Methods

Finite element modeling of femur

A 63-year-old healthy male volunteer of 72 kg was selected for this study, CT scanning was conducted for the upper segment of the femur on both sides (64-layer spiral CT machine), and the bone tissue window scanning was chosen. The thickness of the scan layer is 0.9 mm, the space is 0.9 mm, and the scan length is from 10 cm above the apex of the greater trochanter to the knee joint plane. The scan data is saved in digital imaging and communications in medicine format. This study is a computer-based finite element design study, which does not involve human or animal experiments, so it does not need to go through the ethics committee.

The data of the right femur is used as a sample. The CT data was imported into the Mimics17 system for three-dimensional (3D) modeling, a volume mesh was created, the 3D model was materialized, saved in the Initial Graphics Exchange Specification format, and it was imported into the 3D finite element analysis software (UG8.0).

Hollow cone and "Cross" groove design of the distal femoral prosthesis

With reference to Link's LCU femoral prosthesis, 3D finite element analysis software (UG8.0) is used to build the femoral prosthesis models of the distal hollow cone and distal bottom "cross" groove [Figure 1]. According to the length and width

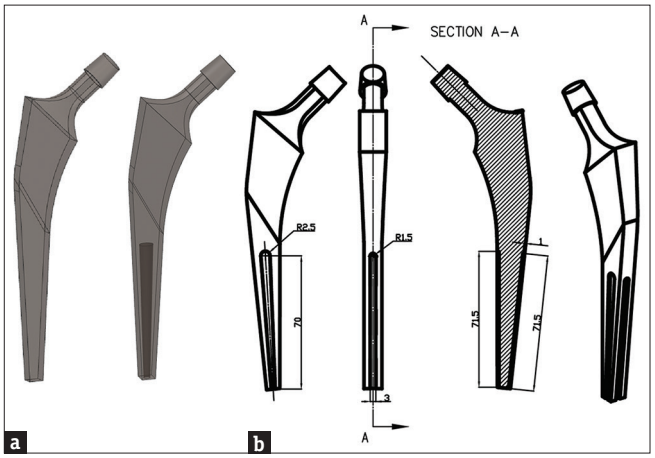

Figure 1: Hollow cone and cross groove design of the distal femoral prosthesis (a) Design drawing of distal taper hole; (b) Design drawing of distal cross groove

Table 1: Unit type and number of each model

Material type	The total number of nodes	The total number of units	Grid type
The femoral prosthesis	370969	256785	C3D10M
Prosthesis without taper holes/MPa	96520	65432	C3D10M
Prosthesis with taper holes/MPa	97263	64937	C3D10M
Length 1:1, groove width 1.0 mm/MPa	105787	70410	C3D10M
Length 1:1, groove width 1.5 mm/MPa	105066	69937	C3D10M
Length 1:1, groove width 2.0 mm/MPa	102719	68291	C3D10M
Length 1:2, groove width 1.0 mm/MPa	104810	70095	C3D10M
Length 1:2, groove 1.5 mm wide/MPa	104652	69953	C3D10M

Table 2: Material properties of femur, prosthesis, and filler.

	Elastic modulus/MPa	Poisson's ratio
The femoral	16700	0.26
The prosthesis	113800	0.34

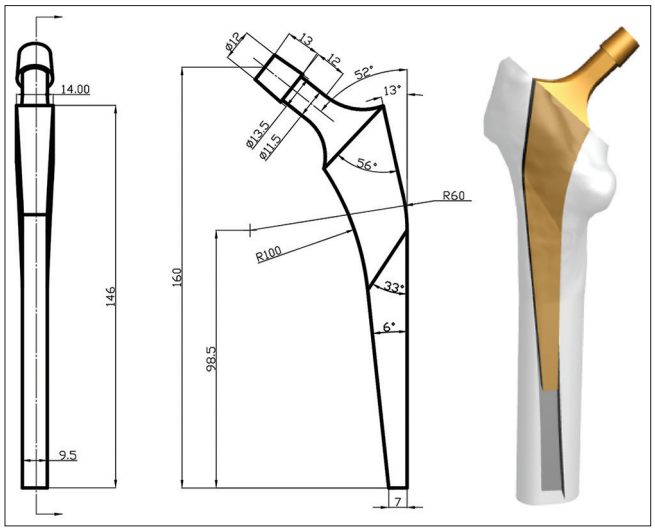

Figure 2: Modeling process of femur and prosthesis

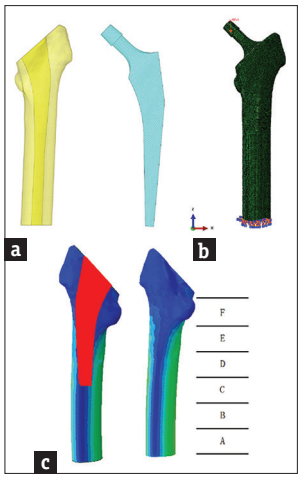

Figure 3: Schematic diagram of simulation analysis of the femoral prosthesis (a) Schematic diagram of femur and prosthesis grid; (b) Schematic diagram of loading and boundary conditions; (c) Results of the femoral partition

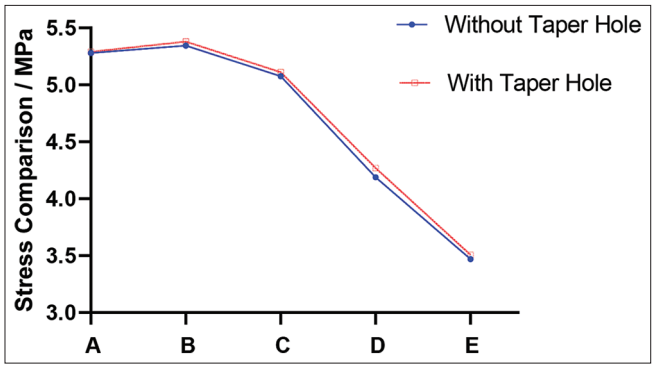

Figure 4: Stress comparison results of the distal prosthesis without and with taper holes

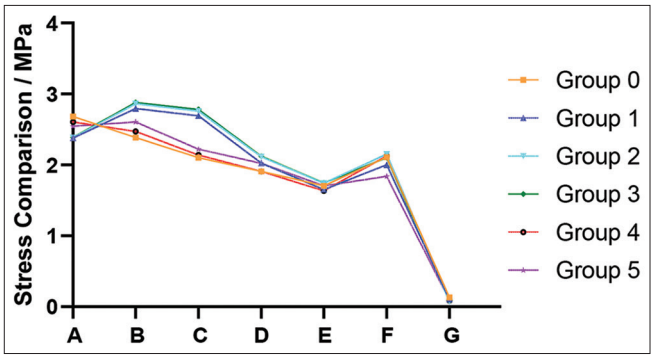

Figure 5: Comparison of zonal stress between the distal and non-slotted femur of the prosthesis

Table 3: Different surface friction coefficient definitions

Contact pair	Friction coefficient
Medial femur–proximal end of prosthesis	0.4
Medial femur–distal prosthesis	0.3

of the "cross" groove at the bottom, they are divided into five groups, namely, group 1 (length 1:1, groove width 1.0 mm); group 2 (length 1:1, groove width 1.5 mm); group 3 (length 1:1, groove width 2.0 mm); group 4 (length 1:2, groove width 1.0 mm); group 5 (length 1:2, groove 1.5 mm wide). And the non-grooved distal femur prosthesis is designated as group 0.

Process of finite element analysis

Modeling

The femoral model is reconstructed based on the CT scan data of the femur, and the 3D prosthesis model is built using the 3D modeling software (UG8.0). The size of the prosthesis model is adjusted appropriately according to the size of the actual prosthesis model, and the 3D assembly model of the prosthesis implanted in the femur is constructed. To simplify the model, the rounded corners where the prosthesis and the femur contacts are ignored [Figure 2].

Meshing

The model built in the previous step was imported into the HyperMesh 10.0 software and used the software to mesh the femur and the prosthesis, respectively. The meshing results are shown in Table 1.

Material properties

In ABAQUS6.14, the material properties of different parts are defined as shown in Table 2.

Definition of contact

The outer surface of the prosthesis stem is in full-friction contact with the inner wall of the femur. Since the upper and lower ends of the prosthesis have different working conditions when in contact with the femur, different contact properties are selected. If there is a filler, then the outer cylindrical surface of the filler is in friction contact with the inner surface of the prosthesis opening, and the circular end face of

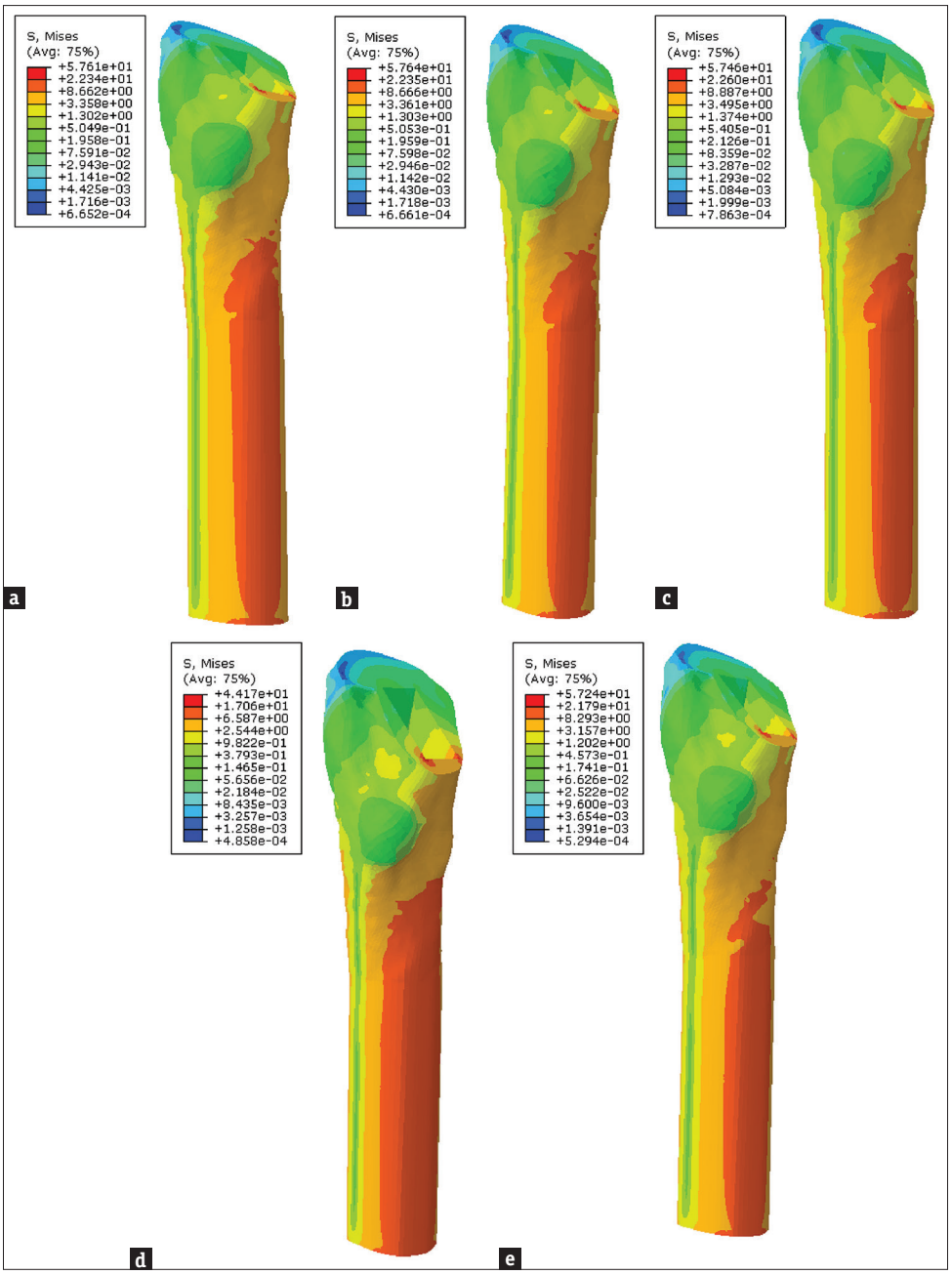

Figure 6: The femoral stress nephogram of the cross-slotted prosthesis. (a) length 1:1, groove width 1.0 mm; (b) length 1:1, groove width 1.5 mm; (c) length 1:1, groove width 2.0 mm; (d) length 1:2, groove width 1.0 mm; (e) length 1:2, groove 1.5 mm wide

the filler is in friction contact with the inner wall of the femur. The friction coefficients of different surfaces are defined as shown in Table 3.

Loading conditions

In practice, the working conditions of the femoral prosthesis model are complex, and the actual measurement is very difficult. The influencing factors of some working conditions are small and it is of little significance to simulate such complicated working conditions with finite element software. Therefore, one working condition is selected for analysis and comparison, that is, the simplified force model of a person standing on one leg of about 75 kg. A reference point on the head of the prosthesis was selected and defined as RP-1, and then coupled this point with the head of the prosthesis. A force of 750 N in the *z*-direction to the reference point RP-1 was applied. A fully-fixed constraint is imposed on the distal femur as the boundary condition as shown in Figure 3.

Submit for Analysis and post-processing

The Steps (3)–(6) are all completed in ABAQUS6.14. The works were directly submitted in the ABAQUS

Table 4: Stress value of each segment of femur under different elastic modulus

	The medial femur						The lateral femur						The anterior femur						The posterior femur					
	A	B	C	D	E	F	A	B	C	D	E	F	A	B	C	D	E	F	A	B	C	D	E	F
Elastic modulus:56900																								
prosthesis without taper holes/MPa	4.39	4.50	4.37	5.03	4.06	3.73	2.05	2.20	2.13	3.16	3.11	1.61	2.14	2.15	2.17	2.67	2.54	2.20	1.63	1.67	1.66	2.27	2.87	2.81
prosthesis with taper holes/MPa	4.39	4.49	4.23	4.72	3.72	3.59	2.05	2.22	2.43	2.65	2.76	1.60	2.14	2.15	2.40	2.36	2.16	2.15	1.63	1.67	1.96	2.03	2.39	2.75
length 1:1, groove width 1.0mm/Mpa	4.39	4.50	4.35	4.98	3.99	3.77	2.05	2.20	2.14	2.83	3.02	1.60	2.14	2.15	2.16	2.58	2.42	2.17	1.63	1.67	1.66	2.24	2.73	2.80
length 1:1, groove width 1.5mm/MPa	4.39	4.50	4.35	4.99	4.00	3.78	2.05	2.20	2.13	2.85	3.03	1.60	2.14	2.15	2.16	2.59	2.43	2.17	1.63	1.67	1.66	2.25	2.74	2.80
length 1:1, groove width 2.0mm/MPa	4.39	4.50	4.36	4.99	4.01	3.78	2.05	2.20	2.13	2.86	3.04	1.60	2.14	2.15	2.16	2.60	2.44	2.18	1.63	1.67	1.66	2.25	2.75	2.80
length 1:2, groove width 1.0mm/MPa	4.39	4.49	4.21	4.71	3.74	3.64	2.05	2.21	2.35	2.68	2.75	1.61	2.14	2.15	2.36	2.41	2.16	2.16	1.63	1.67	1.88	2.06	2.39	2.75
length 1:2, groove 1.5mm wide/MPa	4.39	4.49	4.22	4.72	3.75	3.72	2.05	2.21	2.33	2.68	2.75	1.60	2.14	2.15	2.35	2.41	2.18	2.15	1.63	1.67	1.86	2.06	2.41	2.76
Elastic modulus:113800																								
prosthesis without taper holes/MPa	4.40	4.49	4.12	4.44	3.29	3.02	2.05	2.22	2.75	2.54	2.35	1.35	2.14	2.15	2.72	2.40	1.94	1.89	1.63	1.67	2.30	2.13	2.19	2.33
prosthesis with taper holes/MPa	4.40	4.49	4.14	4.46	3.33	3.03	2.05	2.22	2.71	2.54	2.38	1.35	2.14	2.15	2.69	2.38	1.98	1.88	1.63	1.67	2.27	2.11	2.23	2.36
length 1:1, groove width 1.0mm/Mpa	4.39	4.50	4.33	4.87	3.84	3.25	2.05	2.21	2.16	2.85	2.85	1.35	2.14	2.15	2.15	2.74	2.44	1.93	1.63	1.67	1.67	2.43	2.82	2.41
length 1:1, groove width 1.5mm/MPa	4.39	4.50	4.34	4.88	3.85	3.25	2.05	2.21	2.16	2.88	2.86	1.33	2.14	2.15	2.15	2.76	2.46	1.93	1.63	1.67	1.67	2.45	2.85	2.41
length 1:1, groove width 2.0mm/MPa	4.39	4.50	4.34	4.89	3.87	3.25	2.05	2.20	2.15	2.91	2.89	1.35	2.14	2.15	2.15	2.78	2.48	1.94	1.63	1.67	1.66	2.46	2.88	2.42
length 1:2, groove width 1.0mm/MPa	4.40	4.49	4.11	4.46	3.35	3.10	2.05	2.22	2.64	2.58	2.35	1.35	2.14	2.15	2.64	2.47	1.98	1.90	1.63	1.67	2.16	2.16	2.23	2.36
length 1:2, groove 1.5mm wide/MPa	4.40	4.49	4.12	4.47	3.37	3.16	2.05	2.22	2.62	2.58	2.36	1.34	2.14	2.15	2.62	2.47	1.99	1.89	1.63	1.67	2.13	2.16	2.24	2.36

software, its self-installed functions were used for analysis and processing, and then the results are outputted.

Design analysis results of the distal prosthesis

1. The stress comparison results of the prosthesis without a taper hole and with a taper hole are shown in Figure 4.
2. For the distal cross-grooved prosthesis, the average stress values of stress regions A, B, C, D, E, F, and H are shown in Figure 5.
3. The stress nephogram of cross-grooved prosthesis femur are shown in Figure 6.

Through comparison between groups, it is found that the cross groove design of the distal femur can change the stress distribution of the traditional prosthesis in different regions of the femur. It can reduce the stress on the distal femur of the prosthesis and partially increase the stress distribution on the proximal femur. Wherein, the effect of the groove of the 1:1 length ratio is slightly more obvious than that of the 1:2 length ratio.

Considering that the difference between the elastic modulus of the prosthesis and the femur may lead to a change in the magnitude of stress, we reduced the elastic modulus of the femoral prosthesis by half, from 113800MPa to 56900MPa, and the stress change data is shown in Table 4.

The elastic modulus is divided into two groups by high value and low value, and the stress of the nodes corresponding to the two groups of stress values is subjected to an independent sample *T*-test. The final statistical result shows that in the segment E of the inner femur stress, the stress comparison *P* value of the high-value group and the low-value group of no-cone prosthesis, cone prosthesis, cross-grooved prosthesis (depth 1:2, groove width 1.0 mm), and cross groove prosthesis (depth 1:2, groove width 2.0 mm) is <0.05, and the difference has statistical significance. In segment E of the posterior femur stress, the stress comparison *P* value of the high-value group and the low-value group of no-cone prosthesis is <0.05, and the difference has statistical significance. The comparison *P* values of the high-value group and the low-value group of other stress segments are all >0.05, and the difference has no statistical significance.

Discussion

Aseptic loosening of the artificial hip prosthesis is still an intractable complication after artificial hip replacement.[16] The proximal stress shielding of the femoral prosthesis causes bone loss of the proximal femur, which is considered an important cause of aseptic loosening. The stress concentration of the distal femoral prosthesis is an important factor that causes thigh pain and fractures of the distal prosthesis in the corresponding region after surgery. There are many factors that affect the stress distribution of the femoral prosthesis, including prosthetic materials, mechanical design, and surface treatment.[9,17,18]

There are significant differences between the elastic modulus of the metal implant and the femur, which will cause stress shielding and adjacent bone resorption. By now, great progress has been made in the improvement of prosthetic materials. Relying on more precise anatomy and bionic design, the contact stress is minimized, such as the wide-used near-HA coatings, titanium nitride and other oxide coatings and the application of porous trabecular metal, which exhibits a good survival rate of the femoral prosthesis.[19,20] Despite these improvements, the number of patients requiring revision surgery due to aseptic loosening has not been significantly reduced. The bone growth rate on the surface of the material-host bone is still very limited.[21] Other studies have shown that the surface coating treatment is not reliable due to the absorption and degradation of surface materials. According to Cilla's research, subtle shape changes have little effect on the stress shielding of the prosthesis, but significant changes have a certain impact.[13]

In addition to prosthetic materials and surface treatment, the geometric design of the femoral prosthesis is also the main factor affecting the stress distribution of the prosthesis. According to Suksathien's research, the short stem of the femoral prosthesis provides physiological proximal load transfer and less stress shielding, making it a useful option for the femoral reconstruction.[22-24] Schmidt and Hackenbroch found early that the Cenos hollow stem (Artos) reduced the stress shielding in the intertrochanteric region of the femur and the bone remodeling of the distal femur. With a linear hollow cone stem, the stress shielding performance of Gross and Abel is reduced by 22%.[25] Our research found that the geometric design of the taper hole in the central part of the distal femur cannot effectively improve the stress distribution of the femur, which may be related to the size of the bottom taper hole designed in this group. Research by Abdelaal *et al*.[26] found that increase in the cross-sectional area of the femur by designing the geometry of the femoral stem prosthesis may affect the stress distribution from the proximal femur to the middle of the femur. In this study, we hope to optimize the design of the femoral prosthesis, change the geometric shape to reduce the local stress shielding of the proximal femur, and reduce the distal stress concentration, so as

to reduce the probability of prosthesis loosening and the risk of distal femur pain and fracture, thus extending the service life of the femoral prosthesis.

In this study, for the geometric shape optimal design of the distal femoral prosthesis, 3D finite element analysis software was used to build the femoral prosthesis model with a distal hollow cone and distal "cross" groove at the bottom, so as to conduct finite element analysis on stress conduction under different geometries. The stress difference between the two groups has no statistical significance. Our research proves that the one-third inverted hollow cone design of the distal femur cannot significantly improve the stress distribution of the distal femur and cannot effectively decrease the stress concentration effect of the distal femur. The cross groove design of the distal femur has little effect on the change of stress distribution in the proximal femoral region, but it can slightly reduce the stress of the distal femoral prosthesis (segment A 5%), while the stress in segments B and C of the femoral distribution area has increased significantly. After the improvement, the maximum stress at the distal end has reduced by 20%, and the effect of the groove of length ratio 1:1 is slightly more obvious than that of the 1:2 length ratio. Therefore, the design of the 1:1 length cross groove of the distal femoral prosthesis is more conducive to reducing the excessive stress concentration of the distal femur. There is no significant difference in stress change among the three widths (1.0/1.5/2.0 mm) of the 1:1 length groove. This may be related to the large difference in elastic modulus between the artificial femoral metal prosthesis and the human femur. Taking into account the influence of elastic modulus on the stress, after we halved the elastic modulus of the prosthesis, it is found by comparison that only some femoral segments significantly changed the stress distribution. In the segment E of the inner femoral stress, after the elastic modulus of the no-cone prosthesis, cone prosthesis, cross-grooved prosthesis (depth 1:2, groove width 1.0 mm), and cross groove prosthesis (depth 1:2, groove width 2.0 mm) decreased, the corresponding stress value increased, and the stress values of other groups did not change significantly. This group of studies proves that the change of elastic modulus can partially affect the stress change of the proximal femoral prosthesis, which is also consistent with Saravana's research, in which the stress shielding effect of the proximal femur is reduced by optimizing the elastic modulus distribution of the femoral prosthesis.[27]

In summary, the hollow cone design of the distal femoral prosthesis has no significant effect on the stress distribution of the proximal and distal femur. The design of the "cross" groove on the distal femoral prosthesis can slightly reduce the stress concentration of the distal femoral prosthesis, and the length ratio of the groove will slightly affect the stress distribution of the prosthesis. The optimization of the elastic modulus can also change the local stress distribution and reduce the stress shielding of the proximal femur. Certainly, our research still has some limitations. First, the study only simulated and analyzed the stress conduction of the femoral prosthesis stem under 750 N static load of an adult standing on one foot, without considering the influence of abductor muscle strength and gait on the analysis results. Second, there is no animal experiment for observation and study on the bone histology and imaging of the femoral prosthesis to observe and analyze the bone in growth. In the future, it may be one of the research directions of the femoral prosthesis to study the best elastic modulus of the femoral prosthesis to obtain the optimal stress distribution. We hope that our research can provide some useful basic data for the study of the optimal femoral prosthesis with the best stress distribution, bone growth, and histocompatibility.

Acknowledgements

The authors would like to appreciate Dr. Tingting Xia and Dr. Ning Dai for their contributions to this study.

Financial support and sponsorship

This study was supported by the Youth Science and technology Project of Huqiu District (Grant No: 2019Q014), the National Natural Science Foundation of China (81773439), the Medical Research Project of Jiangsu Commission of Health (Z2021043), and the Clinical Key Diseases' Diagnosis and Treatment of Suzhou (LCZX202135).

Conflicts of interest

There are no conflicts of interest.

References

1. Power FR, Cawley DT, Curtin PD. Simultaneous bilateral total hip arthroplasties in nonagenarians. Ir J Med Sci 2017;186:947-51.
2. Morscher EW. Failures and successes in total hip replacement--why good ideas may not work. Scand J Surg 2003;92:113-20.
3. Shishido T, Tateiwa T, Takahashi Y, Masaoka T, Ishida T, Yamamoto K. Effect of stem alignment on long-term outcomes of total hip arthroplasty with cementless Bi-Metric femoral components. J Orthop 2018;15:134-7.
4. Schmidt A, Batailler C, Fary C, Servien E, Lustig S. Dual mobility cups in revision total hip arthroplasty: Efficient strategy to decrease dislocation risk. J Arthroplasty 2020;35:500-7.
5. Melvin JS, Karthikeyan T, Cope R, Fehring TK. Early failures in total hip arthroplasty -- A changing paradigm. J Arthroplasty 2014;29:1285-8.
6. Sadoghi P, Liebensteiner M, Agreiter M, Leithner A,

Böhler N, Labek G. Revision surgery after total joint arthroplasty: A complication-based analysis using worldwide arthroplasty registers. J Arthroplasty 2013;28:1329-32.
7. Yamako G, Chosa E, Totoribe K, Hanada S, Masahashi N, Yamada N, *et al.* In-vitro biomechanical evaluation of stress shielding and initial stability of a low-modulus hip stem made of β type Ti-33.6Nb-4Sn alloy. Med Eng Phys 2014;36:1665-71.
8. Arabnejad S, Johnston B, Tanzer M, Pasini D. Fully porous 3D printed titanium femoral stem to reduce stress-shielding following total hip arthroplasty. J Orthop Res 2017;35:1774-83.
9. Naito Y, Hasegawa M, Tone S, Wakabayashi H, Sudo A. Minimum 10-Year follow-up of cementless total hip arthroplasty with a 32-mm cobalt-chromium head on highly cross-linked polyethylene and a tapered, fiber metal proximally coated femoral stem. J Arthroplasty 2021;36:647-52.
10. Yamako G, Janssen D, Hanada S, Anijs T, Ochiai K, Totoribe K, *et al.* Improving stress shielding following total hip arthroplasty by using a femoral stem made of β type Ti-33.6Nb-4Sn with a Young's modulus gradation. J Biomech 2017;63:135-43.
11. Maji PK, Roychowdhury A, Datta D. Minimizing stress shielding effect of femoral stem—A review. J Med Imaging Health Inform 2013;3:171-8.
12. Ruben RB, Fernandes PR, Folgado J. On the optimal shape of hip implants. J Biomech 2012;45:239-46.
13. Cilla M, Checa S, Duda GN. Strain shielding inspired re-design of proximal femoral stems for total hip arthroplasty. J Orthop Res 2017;35:2534-44.
14. He S, Zhu J, Zhao J. Finite element analysis on the hollow porous design at the proximal end of cementless femoral prosthesis stem. Niger J Clin Pract 2019;22:1276-80.
15. Mavčič B, Antolič V. Cementless femoral stem fixation and leg-length discrepancy after total hip arthroplasty in different proximal femoral morphological types. Int Orthop 2021;45:891-6.
16. Amanatullah DF, Howard JL, Siman H, Trousdale RT, Mabry TM, Berry DJ. Revision total hip arthroplasty in patients with extensive proximal femoral bone loss using a fluted tapered modular femoral component. Bone Joint J 2015;97-B: 312-7.
17. Park MH, Youn YH, Kang JS, Moon KH. Long-term results of hip arthroplasty using extensive porous-coated stem-A minimum follow-up of 15 years. Geriatr Orthop Surg Rehabil 2019;10:2151459319892787.
18. Ebrahimzadeh A, Jamshidi N. Reducing stress shielding and weight as well as helping to revascularization of the femur by applying honeycomb holes in hip prosthesis. J Mech Med Biol 2019;19:1950051.
19. Hedia HS, Aldousari SM, Timraz HA, Fouda N. Stress shielding reduction via graded porosity of a femoral stem implant. Polym Test 2019;61:695-704.
20. Tanaka A, Kaku N, Tabata T, Tagomori H, Tsumura H. Comparison of early femoral bone remodeling and functional outcome after total hip arthroplasty using the SL-PLUS MIA stem with and without hydroxyapatite coating. Musculoskelet Surg 2020;104:313-20.
21. Miño-Fariña N, Muñoz-Guzón F, López-Peña M, Ginebra MP, Del Valle-Fresno S, Ayala D, *et al.* Quantitative analysis of the resorption and osteoconduction of a macroporous calcium phosphate bone cement for the repair of a critical size defect in the femoral condyle. Vet J 2009;179:264-72.
22. Suksathien Y, Tippimanchai T, Akkrasaeng T, Ruangboon C. Mid-term results of short-stem total hip arthroplasty in patients with Crowe type I and II developmental dysplasia of the hip. Eur J Orthop Surg Traumatol 2021;31:319-25.
23. Hochreiter J, Mattiassich G, Ortmaier R, Steinmair M, Anderl C. Femoral bone remodeling after short-stem total hip arthroplasty: A prospective densitometric study. Int Orthop 2020;44:753-9.
24. Pogliacomi F, Schiavi P, Grappiolo G, Ceccarelli F, Vaienti E. Outcome of short versus conventional stem for total hip arthroplasty in the femur with a high cortical index: A five year follow-up prospective multicentre comparative study. Int Orthop 2020;44:61-8.
25. Schmidt J, Hackenbroch MH. The Cenos hollow stem in total hip arthroplasty: First experiences in a prospective study. Arch Orthop Trauma Surg 1994;113:117-20.
26. Abdelaal O, Darwish S, El-Hofy H, Saito Y. Patient-specific design process and evaluation of a hip prosthesis femoral stem. Int J Artif Organs 2019;42:271-90.
27. Saravana Kumar G, George SP. Optimization of custom cementless stem using finite element analysis and elastic modulus distribution for reducing stress-shielding effect. Proc Inst Mech Eng H 2017;231:149-59.